

# Classical Chaotic Dynamics in Bumpy Stadium Billiards

Adam M. Meier  
Quantum Chaos Group  
Department of Physics  
Washington State University  
Pullman, WA

August 10, 2004

## ABSTRACT

Stadium billiards is a model frequently used in the study of essential properties of chaotic systems. Many dynamical properties can be analyzed relatively explicitly in the stadium to aid in the understanding of more complicated systems such as quantum dots. In order to broaden its applicability, the model is adapted to include the presence of quasi-random time-independent perturbations, equivalent to bumpiness on the bottom of the stadium. The investigation of the adapted Poincare sections and orbit mechanics reveals the high sensitivity of these properties to perturbations and indicates the importance of adapting the stadium in this way for modeling purposes.

# Classical Chaotic Dynamics of Bumpy Stadium Billiards

## 1 Introduction

The stadium billiard model describes the dynamics of a billiard ball confined to a frictionless, stadium-shaped playing table. This system is notable for being classically chaotic, in that a slight change in the initial conditions of the ball may lead to an exponential change in position at some later time, while still being fairly simply structured and easy to conceptualize. For this reason, the stadium has been fairly well analyzed, both classically and semi-classically, in an effort to illuminate more complicated chaotic systems.

One particular area of interest has been the existence of orbits, or periodic trajectories, and their uses in classifying chaotic systems. Because real systems unavoidably have small perturbations affecting their dynamics, it is important to the model's application to understand how this "bumpiness" may influence characteristics of the system such as these highly sensitive orbits. In order to investigate the bumpy stadium billiards model, we first show how to model the bumpy stadium before revealing some graphical results about the nature of the model and discussing our attempts to use numerical methods for orbit finding.

## 2 Adaptation of the Stadium

### 2.1 Standard Stadium Billiards

The stadium billiard model places a ball of size 0 into a region bounded by two semi-circles of radius 1 connected by line segments of length 2 as shown in Fig. 1. A ball is typically then released from an initial position  $\vec{x}$  with coordinants  $x$  and  $y$  and initial momenta  $p_x$  and  $p_y$ , respectively. Then, using Newton's laws, we can calculate in steps the path the ball follows as it travels through the stadium and collides with walls. Collisions with the semi-circles on the ends of the stadium tend to send balls that started with slightly different initial conditions on increasingly different paths, thus creating the chaotic dynamics that makes the model interesting. Because it is very difficult to visualize the four dimensional space made up of the two position and two momentum coordinants, it is standard to specify that we are only interested in where the ball collides with the boundary of the stadium, thus reducing the phase space by one dimension. Now given that the ball must conserve energy, we can restrict our interest to just one specific starting momentum reducing the number of interesting dimensions by one again. The ball's path can now be described by just two coordinants,  $S$  and  $\cos \phi$  where  $S$  is a parametrization of the boundary of the stadium starting at 0 on the furthest left point and proceeding counterclockwise, and  $\phi$  is the angle between the path of the ball and the wall the ball has hit most recently. These coordinants are called Birkhoff coordinants. The Hamiltonian equation which describes the system is given in Eq. 2.1, where  $H$  is the constant energy,  $p_x$  and  $p_y$  are as given above, and  $V(x, y)$  is the potential

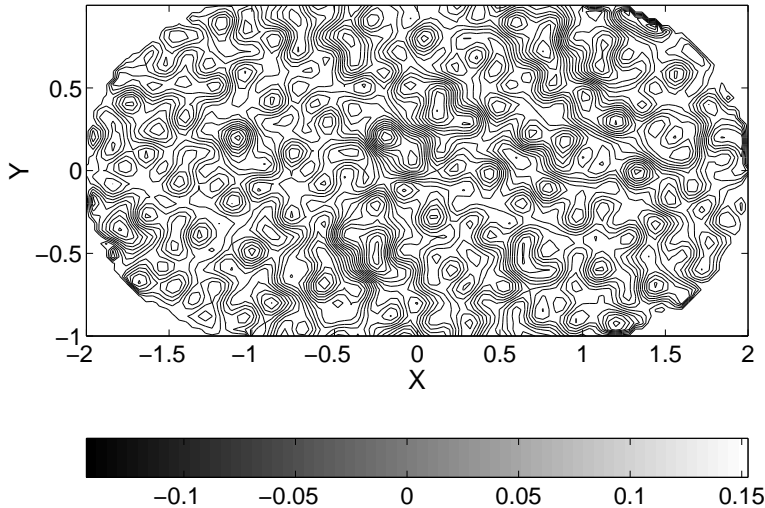


Figure 1: An example of a randomly perturbed stadium. Here the RMS perturbation is .05 times the initial kinetic energy and 10 wave functions have been summed to create the potential.

function which, in the ordinary unperturbed case, is infinite outside of the borders of the stadium and zero inside.

$$H(x, y, p_x, p_y) = \frac{1}{2}(p_x^2 + p_y^2) + V(x, y) \quad (2.1)$$

## 2.2 Adding Bumpiness

In order to study the effects of quasi-random perturbations of the stadium, it was first necessary to determine how to model these perturbations. In order to give seemingly random yet easily differentiable bumps, a potential,  $V_b(x)$ , consisting of a summation of 10 sinusoidal functions of equal amplitude but random wavelength, phaseshift, and direction, all uniformly distributed, was added onto the Hamiltonian of Eq. 2.1. (2.2).

$$V_b(x) = \sum_{k=1}^{10} A \sin \left( \frac{2\pi}{\lambda_k} (\cos(c_k)x + \sin(c_k)y) + \delta_k \right) \quad (2.2)$$

where  $A$  is a common amplitude,  $.2 < \lambda_k \leq 1$  is the wavelength of the  $k^{th}$  wave,  $-\pi \leq \delta_k < \pi$  is the wave's phaseshift, and  $0 \leq c_k < 2\pi$  represents the choice of direction. The effect, as seen in Fig. 1 is to give a smooth but effectively random potential with RMS magnitude chosen to be between .01 and .05 times the initial kinetic energy of the system, very roughly approximating parameters taken from material effects on the bottom of a quantum dot.

Although this potential is not the best approximation possible, it is very convenient in that it is easily modifiable and, more importantly, easily differentiable. This allows for a great deal of control and understanding that might be lost with a more specific model.

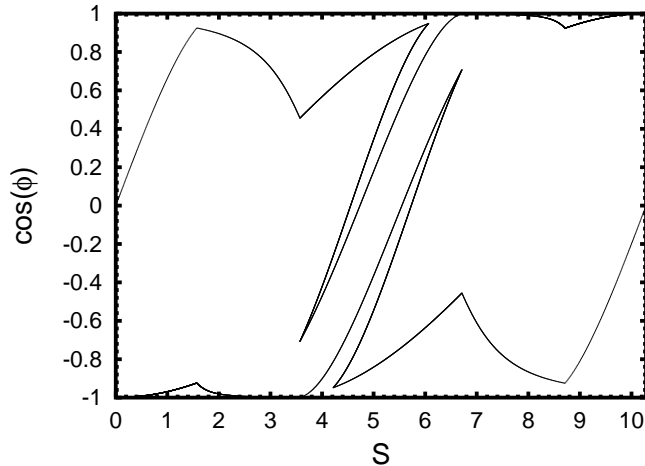


Figure 2: For an unperturbed stadium, the plot of  $F_2(M_0)$ , the location of the second collision with the wall of a point starting on the left hand side of the stadium with angle between 0 and  $\pi$ , for an unperturbed stadium.  $S$  and  $\cos \phi$  are the Birkhoff coordinants described in Sec. 2.1.

### 3 Analysis of Poincare Sections for Bumpy Stadium Billiards

#### 3.1 Definition of Poincare Section

By reducing the phasespace to the two dimensions of  $S$  and  $\cos \phi$ , we may define a map  $F_n(S, \cos \phi)$  (3.3) which gives the intersection of a trajectory with the border of the stadium after  $n$  bounces, which we may then plot easily in two dimensions in what is called a Poincare section.

$$F_n : (S, \cos \phi) \rightarrow (S', \cos \phi') \quad (3.3)$$

If a continuous set of points in the complete phase space is mapped instead by the function that propagates each point for a set amount of time instead of a set number of bounces, then the image space is not continuous since the infinite potential at the boundaries creates a discontinuity in the momentum aspect of that map. However, for  $F_n$  as defined above, it *is* true that a continuous set of points maps to a continuous set of points under  $F_n$ . Due to this property, plots of  $F_n$  are conducive to integration and can be used to give bounds for points of interest, such as intersections between the trajectories of orbits and the surface of section. For these reasons, one important way of characterizing the effects of the perturbations to the stadium model is to investigate the changes in the Poincare section caused by the bumps.

#### 3.2 Results of Adding Perturbations as Seen in Poincare Sections

Figure 2 gives the Poincare section of a typical set  $M_0 \equiv \{(S, \cos(\phi)) : S = 0, 0 \leq \phi < \pi\}$  after 2 bounces in the unperturbed stadium. An intersection of  $M_0$ , seen in this plot as the left-hand border, with  $F_2(M_0)$  represents a possible orbit point, as its final position

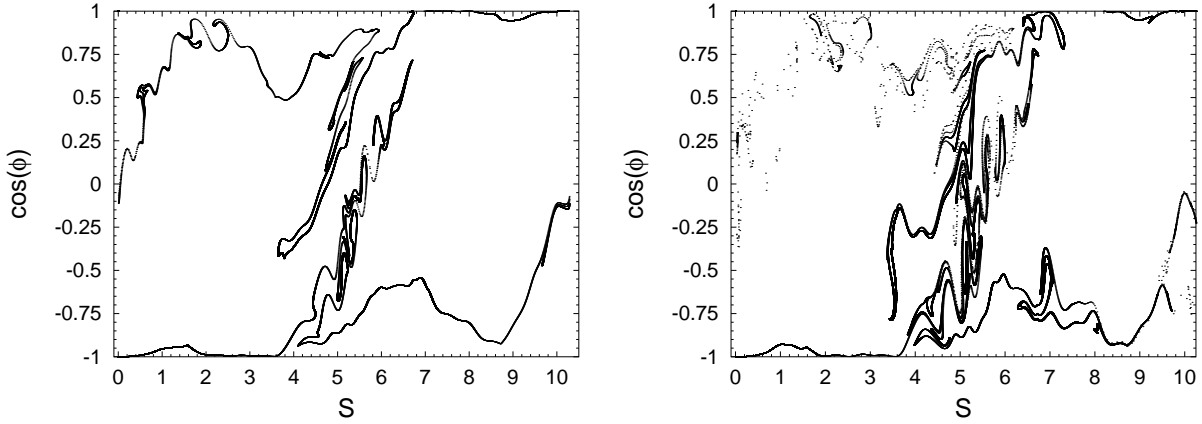


Figure 3: For stadiums perturbed by potentials of RMS magnitude .02 times (left) and .05 times (right) the initial kinetic energy of the system, the plots of  $F_2(M_0)$  as described in Fig. 3.  $M_0$  is exactly the same as in Fig. 3.  $S$  and  $\cos \phi$  are the Birkhoff coordinates described in Sec. 2.1.

in phase space is congruent to one of the initial positions. In contrast, Fig. 3 gives the same section in stadiums perturbed by potentials with RMS magnitudes of .02 and .05 times the initial kinetic energy of the ball on the left and right, respectively. The plots are show a remarkably high sensitivity, more so than was expected from such relatively small perturbations. Specifically, the regions corresponding to collisions with the ends of the stadium show a very high degree of curvature and instability indicative of a highly chaotic system.

Of even greater concern is that there appear to be regions of the solution set, for example in the upper left of the RMS .05 plot of Fig. 3, that are discontinuous with the rest. As mentioned above, discontinuities do not occur in  $F_N(M)$  for the unperturbed stadium, so these regions are cause for concern. On closer inspection, it was discovered that for certain situations such as that depicted in Fig.4 a higher perturbation near a boundary can cause a trajectory to miss a wall that would have been hit by a neighboring trajectory, thus causing all future collisions to occur at radically, and discontinuously, different locations. These near-misses would logically tend to occur for trajectories that have very low angles of approach to a boundary, and, reassuringly, the discontinuities tend to occur precisely in this situation. Further, since a near-miss could occur on the first or any subsequent bounce, the Poincare sections for progressive numbers of bounces become increasingly discontinuous, eventually becoming essentially useless for any sort of analytic task.

Another interesting aspect of the perturbed Poincare section lies in the number of possible orbit points. Closer inspection of the right and left hand sides of the plot reveals that there are a large number of intersections of  $F_2(M_0)$  and  $M_0$ , which in this plot lies on the border of the plot. Since each of these intersections has the potential to represent an orbit point, there is a possibility that the perturbed stadium actually contains a higher number of orbits than the unperturbed stadium. For example, in a simplified case with a simple potential creating a trough along the  $y = 0$  line of the stadium there are a countably infinite number

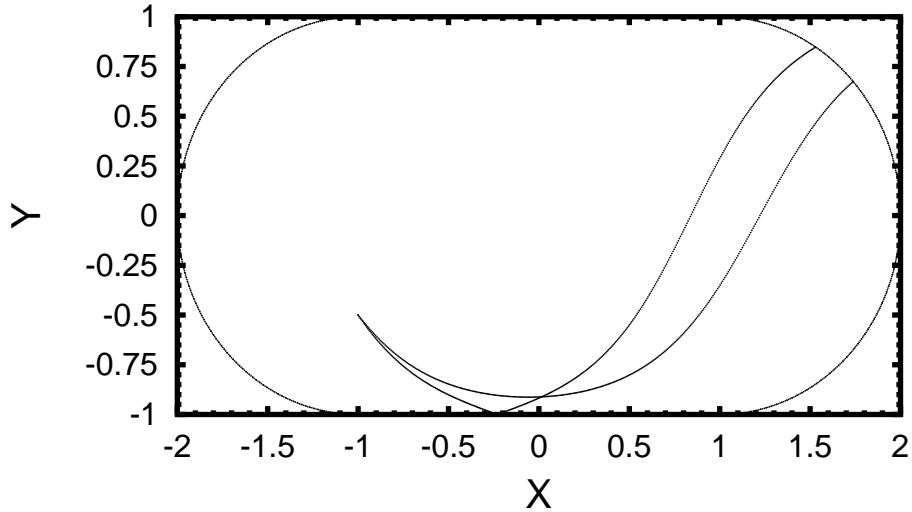


Figure 4: An example of two nearby trajectories exhibiting a near-miss discontinuity. Notice that while the paths are fairly similar the locations of the first bounces for the two trajectories are very different.

of orbits with low energies emanating from the left hand side of the stadium and tracing wave harmonics horizontally. Expanding on this, it is conceivable that such situations occur at least to a limited, probably finite degree in the randomly perturbed stadium. Although the results of Sec. 4 reveal the difficulties in finding any such orbits, the plots lead us to look confidently for their existence.

## 4 Finding Orbits in the Bumpy Stadium

### 4.1 Use of the Stability Matrix to Find Orbits

Although the Poincare sections give a very interesting picture of the qualitative effects of the random potential, a greater level of understanding would be afforded if quantitative results were available as well. The primary method of obtaining such values and, in particular, of calculating locations of orbits is through analysis of the stability matrices of individual trajectories. The stability matrix  $S_M$ , a more in depth discussion and derivation of which can be found in Les Houches...., represents the Jacobian matrix of the map  $G_t : (x, p_x, y, p_y) \rightarrow (x', p'_x, y', p'_y)$  representing the propagation of some initial position  $\vec{x}_0$  for a time  $t$ . The stability matrix then gives a quantitative measure of the chaos of the trajectory by showing how sensitive the final  $p'_y$  is to the initial  $p_y$ , for example. Note that because of the Hamiltonian, area in the phase space is conserved and thus  $S_M$  must have unit determinant. Since the trajectories of interest are often hard to calculate by hand,

numerical methods must be used to approximate  $S_M(\vec{x}, t')$  after some time  $t'$  of the initial point  $\vec{x}$  based on the calculation at  $m$  points along the trajectory of  $K$ , the time derivative operator given in (Eq. 4.4 as described in Heller [2].

$$\frac{dS_M(\vec{x})}{dt} = K(\vec{x}, dt)S_M \quad (4.4)$$

Having calculated  $K$  for each of the  $m$  points along the trajectory, we use equation 4.5 to iterate and find the final stability matrix of interest at some time  $t'$ ; note that  $S_M(\vec{x}, T_0)$  is always equal to  $I$ , the identity matrix, and  $\delta t_n$  is the time step between the  $n$ th point and its predecessor on the trajectory.

$$S_M(\vec{x}, t_n) = S_M(\vec{x}, t_{n-1}) + K(\vec{x}, t_{n-1})S_M(\vec{x}, t_{n-1})\delta t_n \quad (4.5)$$

$$= (I + K(\vec{x}, t_{n-1})\delta t_n)S_M(\vec{x}, t_{n-1}) \quad (4.6)$$

$$S_M(\vec{x}, t') = \prod_{n=0}^m (I + K(\vec{x}, t_{n-1})\delta t_n) \quad (4.7)$$

In the last step we have given a more closed form for the recursion that finally generates the matrix of interest. A correction is needed for collisions with the boundary, when a special matrix ( $M_b$ ) must be inserted into the product to account for the reflection of the trajectory. This matrix, described in 4.8, has been adapted from Tomsovic and Heller [1] to allow for bounces involving non-unity momentum which are unavoidable in the bumpy stadium;  $\phi$  is as defined in Sec. 2.1 and  $p_{\parallel}$  is the momentum parallel to the path of the ball. Here the problem arises that this matrix assumes that  $S_m$  is written in terms of a coordinant system oriented parallel and perpendicular to this path.

$$M_b = \begin{bmatrix} 1 & 0 & 0 & 0 \\ 0 & 1 & 0 & 0 \\ 0 & 0 & -1 & \frac{2p_{\parallel}}{\sin(\phi)} \\ 0 & 0 & 0 & -1 \end{bmatrix} \quad (4.8)$$

This is highly inconvenient for the perturbed stadium, as computation would require a constant change of bases as the path veered through the potential; instead, the old coordinant system in terms of  $x$  and  $y$  is maintained except right before and after a collision, when a rotation matrix is applied to allow the use of  $M_b$ .

Now, assuming that an orbit point  $\vec{x}_o$  exists somewhere near some chosen point  $\vec{x}_i$  in phase space and that the orbit in question involves  $n$  bounces, we find the closest point on the trajectory of  $\vec{x}_i$  to the initial point after  $n$  bounces. Calling this point  $\vec{x}_f$ , we can simplify the process of finding orbit points to finding zeroes of the function  $H(\vec{x}_i)$  (Eq. 4.9).

$$H(x_i) = \vec{x}_f - \vec{x}_i \quad (4.9)$$

If we call the stability matrix of the trajectory at  $x_f$   $S_M$ , then  $\frac{dH(\vec{x}_i)}{d\vec{x}_i}$  is given by equation 4.10 where  $I$  is again the stability matrix.

$$\frac{dH(\vec{x}_i)}{d\vec{x}_i} = S_M - I \quad (4.10)$$

With this knowledge of the function and its derivative, calculation of the orbit point can, at least for the unperturbed stadium, be left to a well developed root-finding algorithm.

## 4.2 Results of Attempts at Orbit Finding in the Bumpy Stadium

Unfortunately, our attempts at orbit finding using the methods of Sec. 4.1 were frustrated by the unpredicted sensitivity of the function  $H(\vec{x})$  as seen manifested in the representative Poincare sections in Sec. 3.2. In particular, the very simplistic root finding methods we used did not account for the discontinuous nature of  $H(\vec{x})$ . Even more sophisticated methods such as Newton-Raphson method assume that the function has a continuous derivative, at least in the region near a root, which is not necessarily true for our model, given the ubiquity of near-miss discontinuities found in  $F_n(\vec{x})$  for higher values of  $n$ . In addition, most root finding methods rely on the assumption that the function is nearly linear in some small region, and as we can extrapolate from the Poincare sections, this region might have to be extremely small for higher bounce number orbits. In fact, although we were able to find orbits involving two bounces fairly regularly in differently perturbed stadiums, an orbit involving three or more bounces proved too elusive. In these situations the calculations would return after each iteration values for  $F_N$  that jumped alternately closer to and further from 0, presumably because the equations led toward locally small values instead of an actual zero, never getting close enough to a real zero for the more quadratic convergence of Newton-Raphson type functions to zoom in on a solution.

There is no reason to believe that the difficulties in discovering orbits indicate that they are less common in the perturbed stadium. Actually, the various shapes of orbits we were able to find involving 2 bounces lead us to believe that there may be just as large a variety of orbits with higher bounce numbers. A more thorough search could be made using more intelligent algorithms for finding the orbits, including at minimum a more tailored root finding method with good global convergence and a better method of choosing initial guesses for the orbit points, possibly using aspects of the Poincare sections to bound a likely region. More drastic changes such as reverting to using stability matrices defined in terms of the basis parallel and perpendicular to the ball's path could also greatly reduce errors in the calculations by removing a difficulty that arises involving trying to invert matrices nearly singular matrices. In addition, this method would allow better comparison to the more thoroughly researched unperturbed stadium billiards, where the stability matrix has already been used extensively to find Lyapunov exponents, which classify the chaos of a system, and other interesting parameters.

## 5 Conclusions

The essential result we hope to convey regarding the effects of bumpiness in stadium billiards is that the bumps do significantly affect the dynamics of the system. With respect to the work that is being done involving orbits and physical applications of the stadium model, we feel that the incorporation of the effects of perturbations must be included in the model, at least as a test to determine what aspects of research will translate well from theory to practice. The Poincare sections in particular deserve more attention, as the specific whorls and regions of high curvature shown in Fig.3 seem to be somewhat common in differently perturbed stadiums. This may indicate that there are some predictable patterns associated with bumpiness that would transcend the specific random perturbations and allow for coher-

ent predictions regarding the dynamics of a system based only on knowledge of some very basic parameters of the perturbations in question.

As described in Sec. 4.2 many avenues also remain to be explored in relation to stability matrices and classification of typical orbits in bumpy stadium models. An more dedicated attempt to study the stability matrices in terms of parallel-path and perpendicular-path elements would likely lead to a closer comparison with the unperturbed stadium, allowing for a better comparison of quantitative descriptions of the two models. Further, given the problems with near-miss discontinuities and highly chaotic regions illustrated in Sec. 3.2, a more tailored root finding algorithm applied to the problem of discovering orbits would likely lead to much more detailed and conclusive results. Perhaps even more interesting would be an attempt add bumps to already developed models that replace the boundaries of the stadium with sudden but continuous functions at the walls; this model could potentially remove the problem of the near-misses and create a still simple, but far more accurate, intermediate step for the bridging of theoretical stadium billiards with physical applications.

## References

- [1] S. Tomsovic and E.J. Heller, "Long-time semiclassical dynamics of chaos: The stadium billiard", *Physical Review E*, vol. 47, no. 1, pp. 282-299 (1993).
- [2] E.J. Heller, "Wavepacket Dynamics and Quantum Chaology" in *Chaos and Quantum Physics*, edited by M.-J. Giannoni, A. Voros, and J. Zinn-Justin, Les Houches Session LII 1989 (Elsevier, Amsterdam, 1991).